

Thermodynamic stability of cis-azobenzene containing DNA thermotropic liquid crystals based on van der Waals force

Lei Zhang,^a Han Liu,^a Yun Liu,^{b*} and Zhongtao Wu^{a*}

^aKey Laboratory of Optic-electric Sensing and Analytical Chemistry for Life Science, MOE; Shandong Key Laboratory of Biochemical Analysis; College of Chemistry and Molecular Engineering, Qingdao University of Science and Technology, Qingdao, 266042, China.

^bGuangdong Key Laboratory for Research and Development of Natural Drugs, Guangdong Medical University, Zhanjiang, 524023, China.

1. General remarks

2. Synthesis of surfactant AZO

3. Synthesis of DNA materials

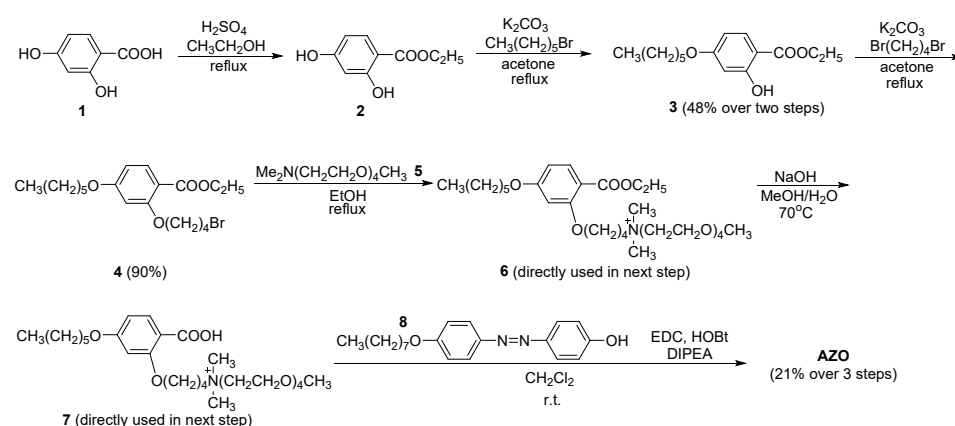
4. Characterizations of surfactant AZO and DNA TLCs

1. General remarks

Materials: the materials used for the preparation of DNA complexes, including DNA (5'-CCTCGCTCTGCTAATCCTGTTA-3', M.W. = 6612.4, 5'-TAACAGGATTAGCAGAGCGAGG-3', M.W. = 6857.5) purchased from Sangon Biotech (Shanghai) Co. Ltd., dioctyldimethylammonium bromide (DOAB) purchased from TCI (Tokyo Chemical Industry Co., Ltd), were used directly without further purifications. All the solutions were prepared using ultrapure water through a Millipore Milli-Q 185 water purification system (Millipore, USA).

Characterizations of AZO and DNA materials: TGA was carried out using a Netzsch STA 449C thermal analyzer in a nitrogen atmosphere and with a heating/cooling rate of 10 °C min⁻¹. DSC was performed by a Netzsch DSC204F1 machine with a heating rate of 5 °C min⁻¹. POM was conducted on a Nikon ECLIPSE LV100NPOL machine with a computational controlled heating plate. SAXS was performed by employing a conventional X-ray source with radiation wavelength of $\lambda = 1.54 \text{ \AA}$. The sample holder is a metal plate with a small hole (diameter $\approx 0.5 \text{ cm}$, thickness $\approx 0.5 \text{ cm}$), where the X-ray beam passes through and the sample-to-detector distance was 18 cm. The scattering vector q is defined as $q = 4\pi \sin\theta/\lambda$ with 2θ being the scattering angle. Rheology was investigated by a Discovery HR-2 hybrid rheometer (TA instruments-Waters LLC, USA). The viscoelastic properties were determined by an oscillatory measurement from 0.01 to 20 Hz. The UV-Vis absorption spectra were recorded on a Shimadzu UV-2600 UV-Vis spectrophotometer, and all the related studies were carried out on fast scan mode with slit widths of 1.0 nm, using matched quartz cells. Test solutions were 200 μL . All absorption scans were saved as ACS II files and further processed in OriginLab software to produce all graphs shown. The wavelengths of UV and Vis photoirradiations are 365 nm (32 mW cm⁻²) and 520 nm (96 mW cm⁻²), respectively.

2. Synthesis of surfactant AZO



Scheme S1. Synthesis of AZO.

The synthetic route from **1** to **4** was followed a reported work:¹

Ethyl 2,4-dihydroxybenzoate (2): To a solution of 2,4-dihydroxybenzoic acid **1** (10 g, 64.88 mmol) in ethanol (50 mL) was added H₂SO₄ (2.0 mL) dropwisely. The resulted mixture was

refluxed overnight. The mixture was cooled to room temperature and the pH was adjusted to 5~6 by adding saturated NaHCO₃ (aq). The mixture was extracted with Et₂O, and the combined organic layers were dried over Na₂SO₄, concentrated in vacuo. The residue was purified by a quick column chromatography on silica gel (petroleum ether/EtOAc = 8 : 1) and put into use directly.

Ethyl 4-(hexyloxy)-2-hydroxybenzoate (3): To a solution of **2** (6.0 g, 32.93 mmol) in acetone (40 mL) were added 1-bromohexane (5.55 mL, 39.53 mmol, 1.2 eq) and K₂CO₃ (13.66 g, 98.84 mmol, 3 eq). The resulted mixture was refluxed over 24 h. After cooling to r.t., the mixture was concentrated in vacuo and subsequently dissolved in CHCl₃. The mixture was filtered and the filtrate was concentrated in vacuo. The residue was purified by column chromatography on silica gel (petroleum ether/EtOAc = 6 : 1) to afford **3** (6.23 g, 48% yield) as a white crystal. ¹H NMR (500 MHz, CDCl₃) δ 11.05 (s, 1 H), 7.73 (d, *J* = 9.5 Hz, 1 H), 6.43-6.41 (m, 2 H), 4.37 (q, *J* = 7.0 Hz, 2 H), 3.97 (t, *J* = 6.5 Hz, 2 H), 1.80-1.75 (m, 2 H), 1.46-1.43 (m, 2 H), 1.39 (t, *J* = 7.0 Hz, 3 H), 1.34-1.33 (m, 4 H), 0.90 (t, *J* = 6.5 Hz, 3 H).

Ethyl 2-(4-bromobutoxy)-4-(hexyloxy)benzoate (4): To a solution of **3** (5.0 g, 18.77 mmol) in acetone (30 mL) were added 1,4-dibromobutane (2.69 mL, 22.53 mmol, 1.2 eq) and K₂CO₃ (3.89 g, 28.15 mmol, 1.5 eq). The resulted mixture was refluxed over 24 h. After cooling to r.t., the mixture was filtered and the filtrate was concentrated in vacuo. The residue was purified by column chromatography on silica gel (petroleum ether/EtOAc = 10 : 1) to afford **4** (6.78 g, 90% yield) as colorless oil. ¹H NMR (400 MHz, CDCl₃) δ 7.82 (d, *J* = 8.4 Hz, 1 H), 6.48-6.43 (m, 2 H), 4.31 (q, *J* = 7.2 Hz, 2 H), 4.03 (t, *J* = 6.0 Hz, 2 H), 3.97 (t, *J* = 6.4 Hz, 2 H), 3.50 (t, *J* = 6.4 Hz, 2 H), 2.16-2.10 (m, 2 H), 2.02-1.95 (m, 2 H), 1.80-1.73 (m, 2 H), 1.48-1.41 (m, 2 H), 1.37-1.31 (m, 7 H), 0.92-0.88 (t, *J* = 7.2 Hz, 3 H).

(E)-N-(4-(5-(hexyloxy)-2-((4-(4-

(octyloxy)phenyl)diazanyl)phenoxy)carbonyl)phenoxy)butyl)-N,N-dimethyl-2,5,8,11-

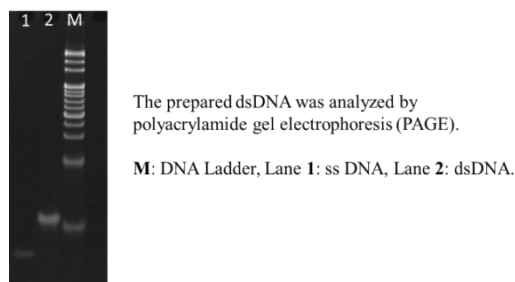
tetraoxatridecan-13-aminium (AZO): to solution of **4** (4.0 g, 9.97 mmol) in CH₃CN (15 mL) was added **5** (2.11 g, 8.97 mmol, 0.9 eq). The resulted mixture was refluxed over 24 h. After cooling to r.t., the mixture was concentrated in vacuo, and the residue **6** was put into next step without further purification. To a solution of **6** in MeOH/H₂O (30 mL, 10:1) was added sodium hydroxide pellets (1.0 g, 25.00 mmol, 2.6 eq). The resulted mixture was refluxed over 12 h. After cooling to r.t., the mixture was acidified to pH ~2-4 by HCl (conc., 12 M). The mixture was concentrated in vacuo to remove the MeOH and the residue was extracted with CHCl₃, and the organic layer was separated, dried and concentrated in vacuo. The residue **7** was put into next step without further purification. To a solution of **7** in dry CH₂Cl₂ (15 mL) were added **8** (3.25 g, 9.97 mmol, 1.0 eq), EDC (1.90 g, 9.97 mmol, 1.0 eq), HOBt (1.35 g, 9.97 mmol, 1.0 eq) and DIPEA (1.65 mL, 9.97 mmol, 1.0 eq). The resulted mixture was stirred at r.t. over 24 h. The filtrate was concentrated in vacuo and subsequently purified by column chromatography on silica gel (EtOAc/EtOH/H₂O = 6 : 4 : 1) twice to afford **AZO** (1.92 g, 21% yield over 3 steps) as yellow oil. It is worth noting that a small amount of **5** and **8** could not be separated from **AZO**, due to their strong molecular interactions with **AZO**. The mass concentration of **AZO** in 95% could be calculated according to ¹H NMR analysis.

Note: **5** and **8** were prepared following a reported procedure from us.²

¹H NMR (500 MHz, CDCl₃) δ 8.05 (d, *J* = 9.0 Hz, 1 H), 7.90 (d, *J* = 9.0 Hz, 2 H), 7.87 (d, *J* = 9.0 Hz, 2 H), 7.25 (d, *J* = 9.5 Hz, 2 H), 6.98 (d, *J* = 9.0 Hz, 2 H), 6.53 (dd, *J* = 9.0, 2.0 Hz, 1 H), 6.47

3. Synthesis of DNA melts

DNA-AZO (1:5): the aqueous solution of ssDNA (10 mM MgCl₂, 50 mM NaCl, and 10 mM Tris-HCl, pH 7.5) with sequence of (5'-CCTCGCTCTGCTAATCCTGTTA-3') (2 mM) and aqueous solution of ssDNA with sequence of (5'-TAACAGGATTAGCAGAGCGAGG-3') (2 mM) were mixed together. The mixture was heated to 90 °C for 15 min and cooling down to room temperature slowly to form the needed double stranded DNA. The formation of double stranded DNA was confirmed by the PAGE analysis, see below.



The aqueous solution of AZO (23.6 mM, 186.4 μL) was added into the aqueous double stranded DNA solution (1 mM, 20 μL) using a pipette, which leads to a mixture of ~5 mol of surfactants with 1 mol of phosphate group within DNA. The resulted mixture became cloudy because of the formation of DNA-AZO precipitate. After a centrifugation, the aqueous supernatant was removed, leaving the precipitate at the bottom of vial. The precipitate was washed with Milli-Q water, centrifuged, and separated from the aqueous supernatant for a further purification in twice. The final obtained precipitate was lyophilization to afford the needed DNA-AZO (1:5) TLC.

DNA-AZO-DOAB: DNA-AZO-DOAB (1:x:y) was prepared following a procedure as that of DNA-AZO (1:5), but using AZO (23.6 mM, 149 μL) and DOAB (65 mM, 13.5 μL) for DNA-AZO-DOAB (1:4:1), AZO (23.6 mM, 112 μL) and DOAB (65 mM, 27 μL) for DNA-AZO-DOAB (1:3:2), AZO (23.6 mM, 74.6 μL) and DOAB (65 mM, 40.5 μL) for DNA-AZO-DOAB (1:2:3), AZO (23.6 mM, 37.3 μL) and DOAB (65 mM, 54 μL) for DNA-AZO-DOAB (1:1:4), respectively.

4. Characterizations of surfactant AZO and DNA TLCs

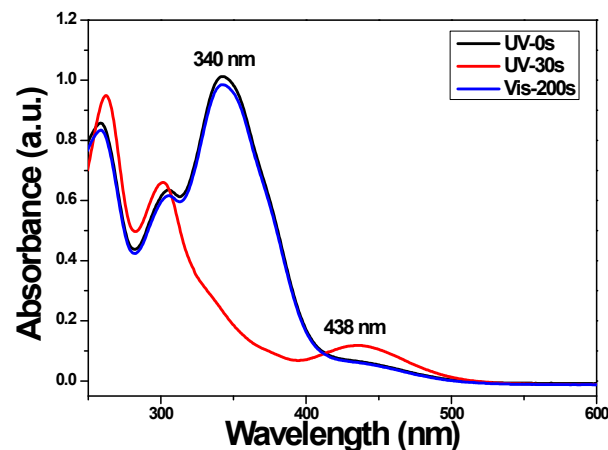


Figure S1. UV-Vis absorption spectra changes of aqueous solution of AZO (60 μM) under UV

and Vis light at r.t..

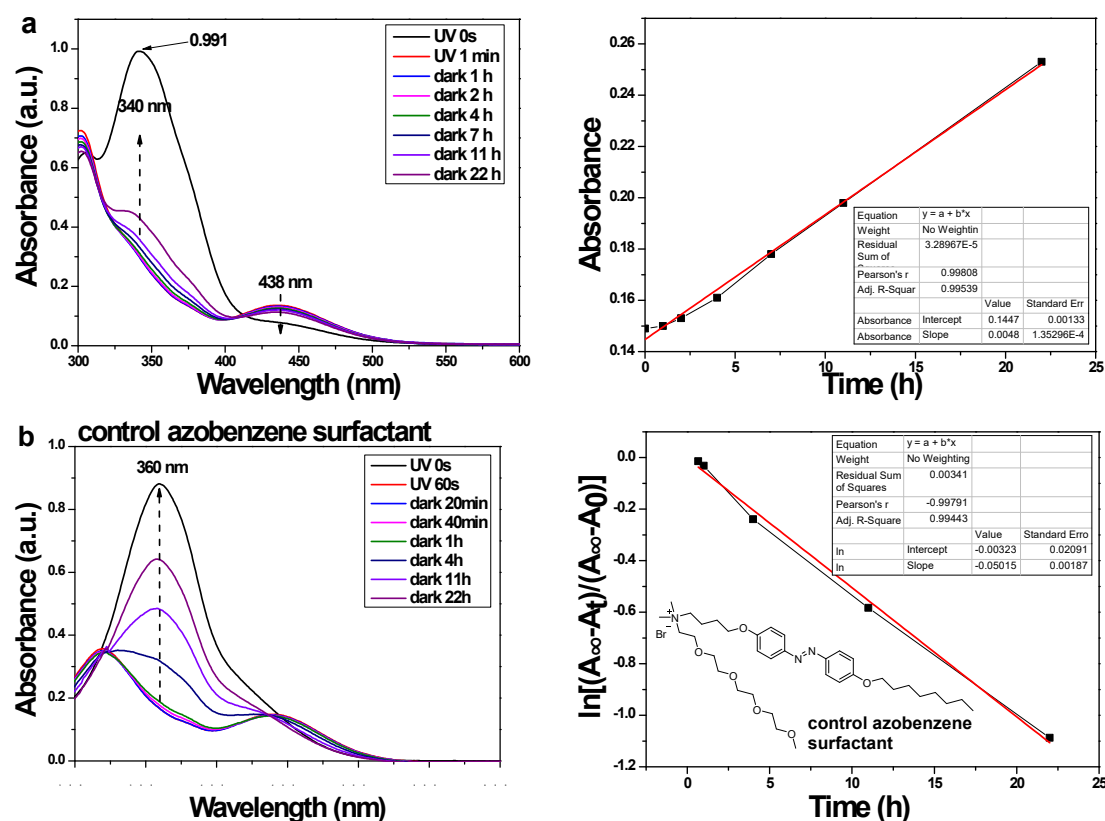


Figure S2. a) Time-dependent UV-Vis absorption spectral changes of AZO in aqueous solution (60 μM) at r.t. under firstly UV light irradiation over 1 min and then storing in dark. The maximum absorption peak at 340 nm for $\pi\text{-}\pi^*$ absorption is used for drawing the plotted graphs. The absorbance at 340 nm with time is fitted by a single-exponential function as $A = 0.1448 + 0.0048 \cdot t$. An assumption that the thermodynamic *cis-trans* isomerization of AZO fits such a single-exponential function within the half-life period is used for determining the half-life of *cis*-AZO under dark condition at r.t.. Therefore, $0.991/2 = 0.1447 + 0.0048 \cdot t_{1/2}$ provides the half-life of *cis*-AZO with ~ 71.4 h.

b) Time-dependent UV-Vis absorption spectral changes of control azobenzene surfactant in aqueous solution (60.0 μM) at r.t. under firstly UV light over 60 s and then in dark. The control azobenzene surfactant was synthesized by following the reported procedure from us.² The maximum absorption peak at 360 nm for $\pi\text{-}\pi^*$ absorption is used for drawing the plotted graph. Equation of $\ln[(A_\infty - A_t)/(A_\infty - A_0)] = -\kappa_{rev} t$ is used for obtaining the thermodynamic *cis-trans* isomerization rate of AZO, $\kappa_{rev} = 0.05015 \text{ h}^{-1}$, and $t_{1/2} = \ln 2 / \kappa_{rev}$ is used for obtaining the half-life of AZO, $t_{1/2} = \ln 2 / 0.05015 = 13.82$ h. A_∞ is the absorption intensity of *trans*-AZO rich state before UV illumination. A_t is the absorption intensity of AZO at "t" time. A_0 is the absorption intensity of *cis*-AZO rich state after UV irradiation.

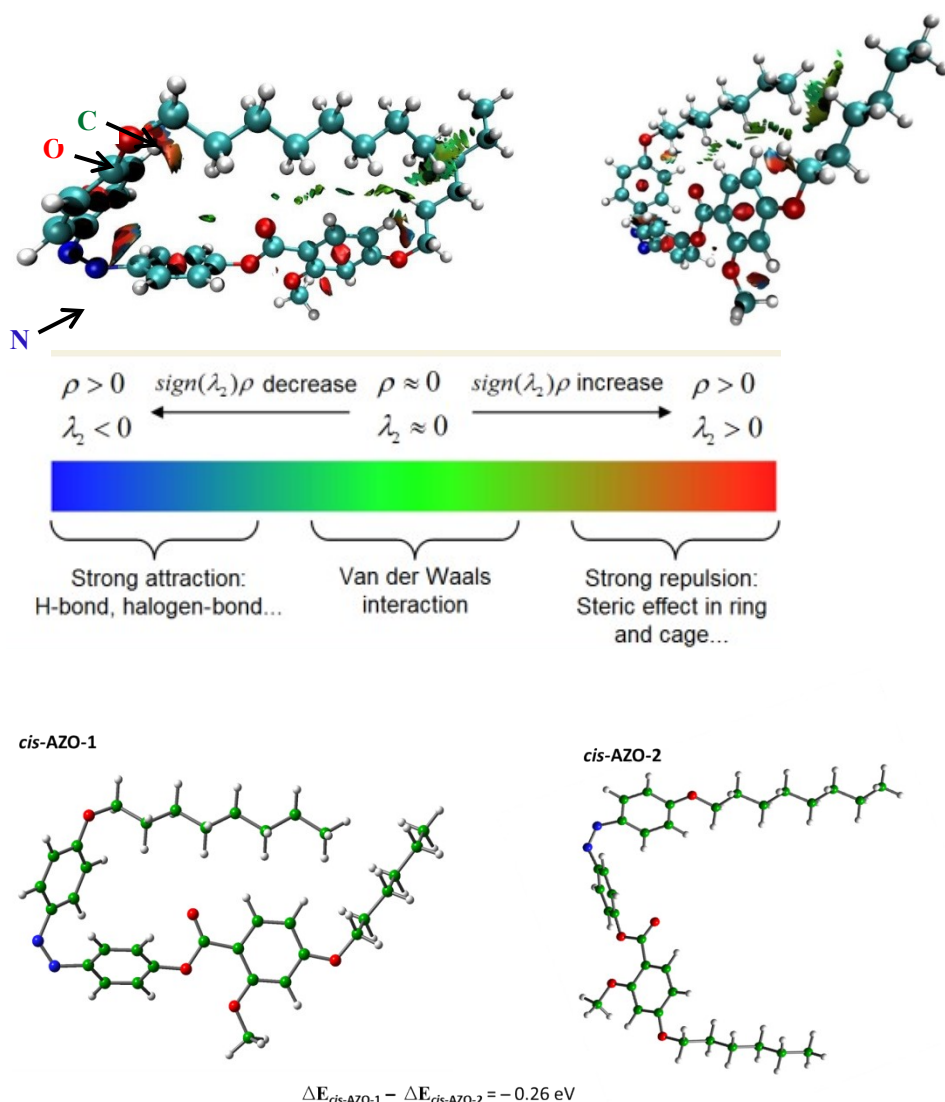


Figure S3. Different perspective images on the visualization of van der Waals interaction between the two alkyl chains, which can be achieved from the *cis*-isomer of AZO through the reduced density gradient (RDG) calculation based on the electron density of *cis*-AZO³⁻⁴. As depicted, the low-density and low gradient region in *cis*-AZO mainly corresponds to the non-bounded overlaps between alkyl chains, which are originated from van der Waals interaction. The geometric optimizations of the proposed states of *cis*-AZO were performed within Gaussian 16 program package (Revision D.01)⁵ at the level of density functional theory (DFT) B3LYP functional⁶ coupled with Grimme D3 dispersion correction⁷ and 6-31G (d, p) basis set. To confirm the nature of obtained minima, vibrational frequency calculations were then carried out at the same level of theory as geometric optimizations. It is conceivable that, the AZO molecules investigated here should have several possible conformations, in particular the alkyl chains of *cis*-AZO. Two possible conformations of *cis*-AZO-1 and *cis*-AZO-2 have been optimized using the hybrid B3LYP functional coupled with the 6-31G (d,p) basis set. With the same theory level, frequency analysis was performed to confirm the nature of obtained minima, and it is shown that *cis*-AZO-1 is more stable with lower relative energies than *cis*-AZO-2.

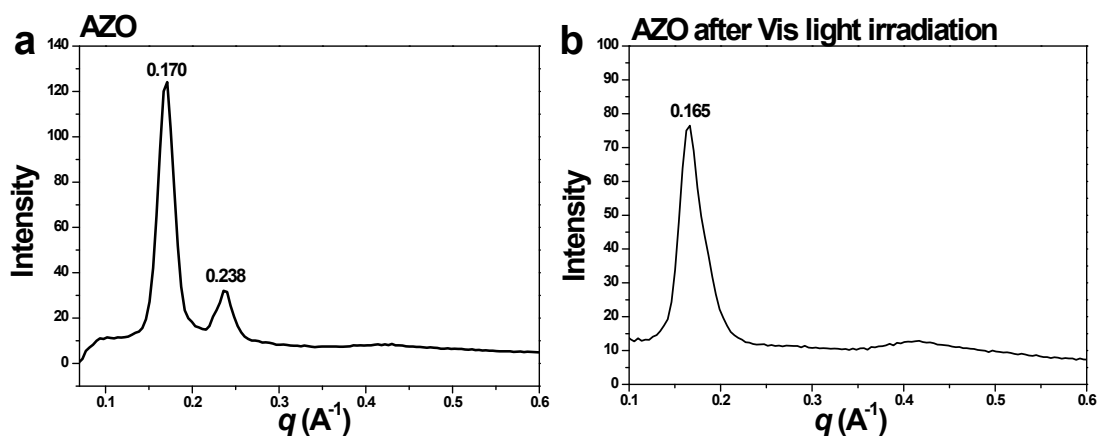


Figure S4. SAXS profiles of AZO a) before and b) after Vis light irradiation at room temperature. Pristine AZO gives peaks at 0.170 Å and 0.238 Å, corresponding to the d -spacing distances of 3.69 nm and 2.64 nm. Here, we attribute these two peaks to *trans*-AZO and *cis*-AZO, which could be confirmed by the disappearance of *cis*-AZO peak after treating AZO with Vis light. *trans*-AZO and *cis*-AZO are in nematic arrangement by showing no following harmonics, respectively. A layer spacing difference of 1.05 nm is much larger than the the length change of 0.35 nm between *trans*-azobenzene and *cis*-azobenzene.⁸ This phenomenon is caused by the different positionings of two alkyl chains in the conformation of *trans*-AZO and *cis*-AZO, reffering to the extended positioning in *trans*-AZO and closed positioning in *cis*-AZO (this also gives an indirect evidence for the interaction between two alkyl chains).

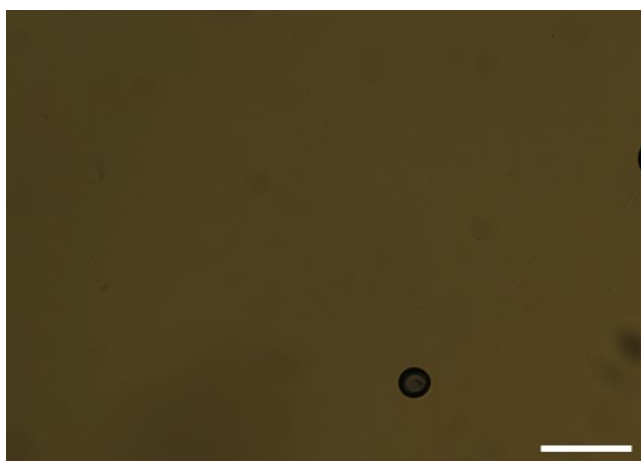


Figure S5. POM picture of the isotropic liquid state of DNA-AZO-DOAB (1:1:4). The scale bar is 50 μm .

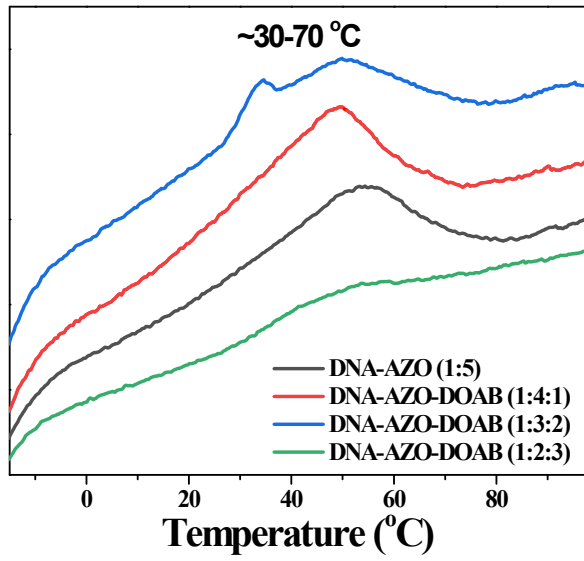


Figure S6. DSC profiles of DNA-AZO-DOAB TLCs.

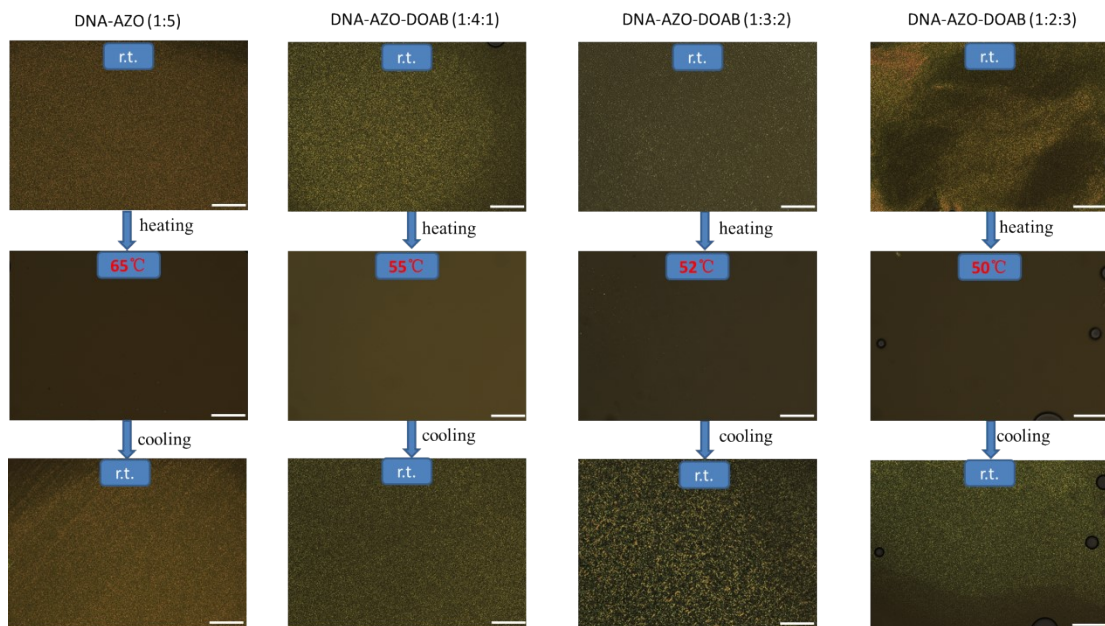


Figure S7. A summary on the temperature-dependent POM analysis of DNA TLCs. The scale bar is 50 μm .

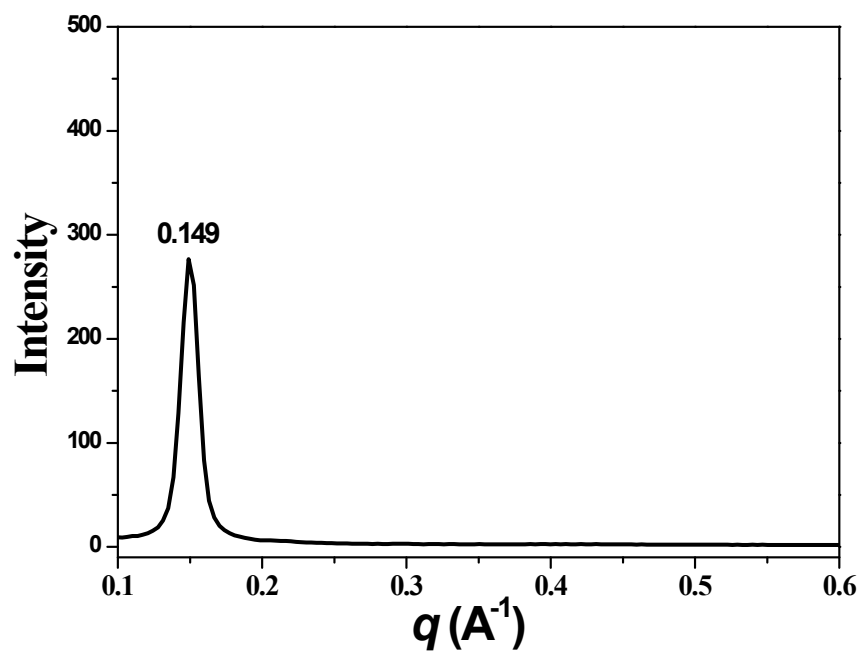


Figure S8. SAXS profile of ssDNA-AZO (1:5) at room temperature.

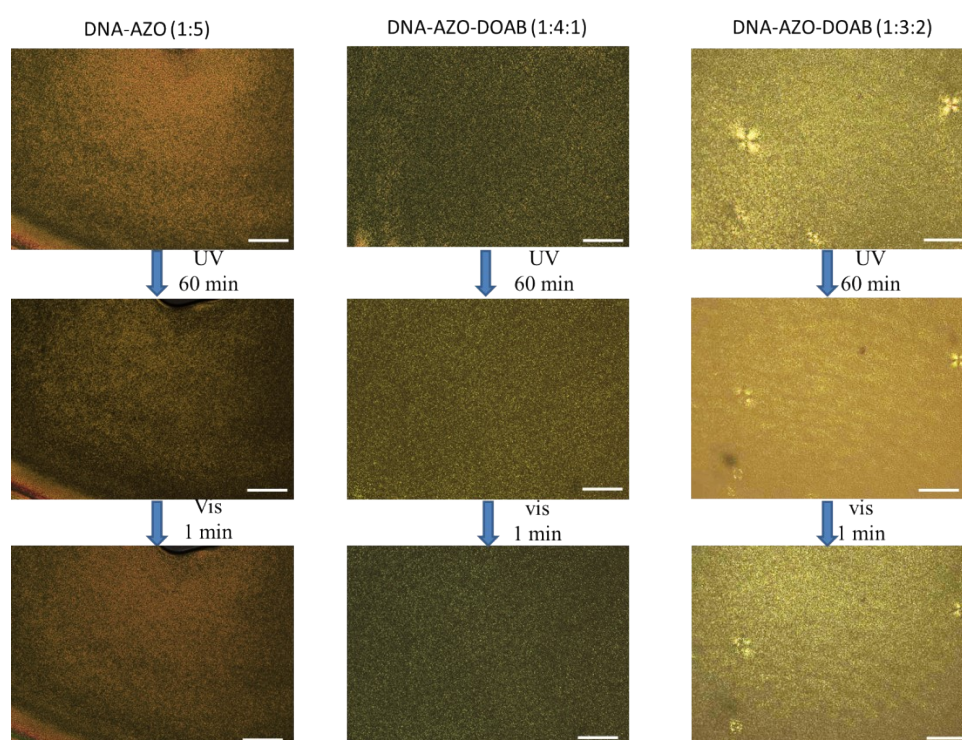


Figure S9. A summary on the light-induced phase transitions of DNA-AZO (1:5), DNA-AZO-DOAB (1:4:1), DNA-AZO-DOAB (1:3:2) at r.t., recorded by POM. The scale bar is 50 μm .

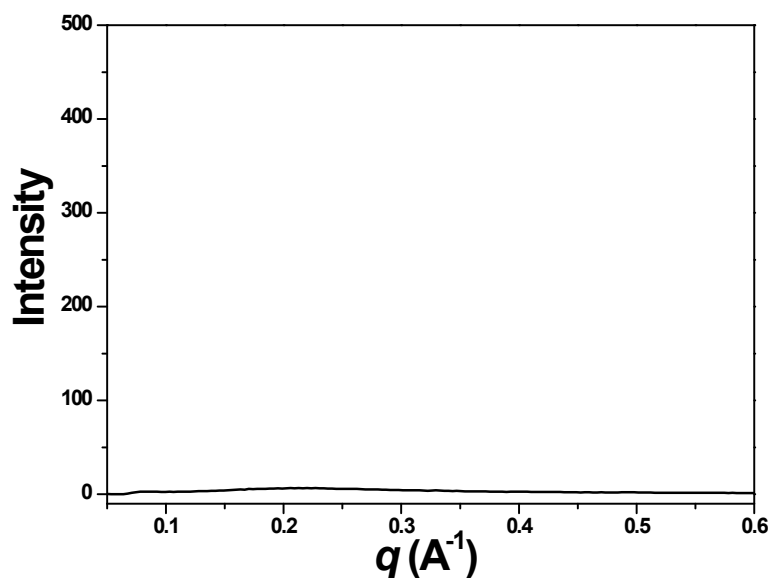


Figure S10. SAXS profile of DNA-AZO-DOAB (1:2:3) after UV illumination at r.t..

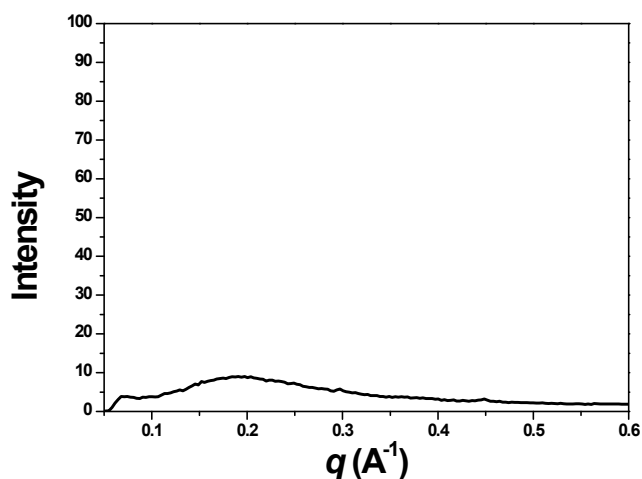


Figure S11. The SAXS profile of DNA-AZO-DOAB (1:2:3) after subsequent UV and Vis light illuminations at r.t.. A broad peak at $\sim 0.195 \text{ \AA}^{-1}$ with low intensity was observed, indicating a recovery of nematic ordered structure but not to the original state.

References

1. L. Zhang, S. Maity, K. Liu, Q. Liu, R. Göstl, G. Portale, W. H. Roos and A. Herrmann, *Small*, 2017, **13**, 1701207.
2. L. Zhang, Z. Tang, L. Hou, Y. Qu, Y. Deng, C. Zhang, C. Xie and Z. Wu, *Analyst*, 2020, **145**, 1641-1645.
3. E. R. Johnson, S. Keinan, P. Mori-Sánchez, J. Contreras-García, A. J. Cohen, W. Yang, *Journal of the American Chemical Society*, 2010, **132**, 6498-6506.
4. T. Lu, F. Chen, *Journal of Computational Chemistry*, 2012, **33** (5), 580-592.
5. M. J. Frisch, G. W. Trucks, H. B. Schlegel, G. E. Scuseria, M. A. Robb, J. R. Cheeseman, G.

Scalmani, V. Barone, B. Mennucci, G. A. Petersson, H. Nakatsuji, M. Caricato, X. Li, H. P. Hratchian, A. F. Izmaylov, J. Bloino, G. Zheng, J. L. Sonnenberg, M. Hada, M. Ehara, K. Toyota, R. Fukuda, J. Hasegawa, M. Ishida, T. Nakajima, Y. Honda, O. Kitao, H. Nakai, T. Vreven, J.A. Montgomery, J. E. Peralta, F. Ogliaro, M. Bearpark, J. J. Heyd, E. Brothers, K. N. Kudin, V. N. Staroverov, T. Keith, R. Kobayashi, J. Normand, K. Raghavachari, A. Rendell, J. C. Burant, S. S. Iyengar, J. Tomasi, M. Cossi, N. Rega, M. J. Millam, M. Klene, J. E. Knox, J. B. Cross, V. Bakken, C. Adamo, J. Jaramillo, R. Gomperts, R. E. Stratmann, O. Yazyev, A. J. Austin, R. Cammi, C. Pomelli, J. W. Ochterski, R. L. Martin, K. Morokuma, V. G. Zakrzewski, G. A. Voth, P. Salvador, J. J. Dannenberg, S. Dapprich, A. D. Daniels, Ö. Farkas, J. B. Foresman, J. V. Ortiz, J. Cioslowski, D. J. Fox, 09 Gaussian, Revision D.01, Gaussian, Inc., Wallingford, CT, 2013.

6. A.D. Becke, *Journal of Chemical Physics*, 1993, 98 (7), 5648-5652.
7. S. Grimme, S. Ehrlich, L. Goerigk, *Journal of Computational Chemistry*, 2011, 32 (7), 1456-1465.
8. E. Merino and M. Ribagorda, *Beilstein Journal of Organic Chemistry*, 2012, 8, 1071-1090.